Available online at www.sciencedirect.com

SCIENCE DIRECT®

Journal of volcanology and geothermal research

ELSEVIER

Journal of Volcanology and Geothermal Research 143 (2005) 237–257

www.elsevier.com/locate/jvolgeores

Correlation and petrogenesis of silicic pyroclastic rocks in the Northern Pannonian Basin, Eastern-Central Europe: In situ trace element data of glass shards and mineral chemical constraints

Szabolcs Harangi[a,*], Paul R.D. Mason[b], Réka Lukács[a,c]

[a]*Department of Petrology and Geochemistry, Eötvös University, H-1117 Budapest, Pázmány Péter sétány 1/C, Hungary*
[b]*Vening Meinesz Research School of Geodynamics, Department of Earth Sciences, Utrecht University, Budapestlaan 4, 3584 CD Utrecht, The Netherlands*
[c]*Institute of Earth Sciences, Geozentrum, University of Vienna, Althanstrasse 14, A-1090 Vienna, Austria*

Received 8 September 2003; accepted 19 November 2004

Abstract

The Neogene volcanism of the Carpathian–Pannonian Region, Eastern-Central Europe started with repeated explosive eruption of silicic magmas. Volcanic products consist mostly of non-welded and partially to densely welded ignimbrites, which cover large areas in the Pannonian Basin. Since this volcanism occurred during a long time interval, from 21 Ma to 13.5 Ma ago, these pyroclastic deposits have great stratigraphic importance, as well as providing valuable information about petrogenetic processes during the formation of the back-arc basin area. In this study, we used in situ trace element data of glasses (glass shards, pumice and fiamme glass) determined by laser ablation inductively coupled plasma mass spectrometry (LA-ICP-MS), combined with microprobe geochemical data of the main mineral phases (plagioclase, biotite), to correlate the scattered outcrops of the ignimbrite units. Based on these data, we distinguished four ignimbrite units in the Bükkalja Volcanic Field, Northern Pannonian Basin. Each of these units is characterized by specific geochemical fingerprints. Thorium, Nb, Y and the rare earth elements are the most effective discriminator elements in glasses. The modal composition of mineral phases (occurrence or lack of certain minerals) and chemistry of plagioclases and biotites are also good correlation tools, especially the Fe, Mg and Ti contents of biotites. We suggest that these correlation criteria, particularly the grain-specific LA-ICP-MS data, could be effectively used also in other ignimbrite fields and in wider tephrochronological studies. The in situ trace element composition of glasses, representing the liquid part of the erupted magma, can be also used to constrain the petrogenesis of the rhyolitic magmas. Trace element ratios such as La/Nb, La/Y and Th/Nb suggest the importance of minor (e.g., hornblende and ilmenite) and accessory (e.g., zircon, allanite) minerals controlling the composition of the erupted melt. Rhyolitic magmas probably evolved from metaluminous andesitic parental melts via fractional crystallization. Syn-eruptive magma mingling was

* Corresponding author. Tel.: +36 12090555x8355; fax: +36 13812108.
E-mail address: szabolcs.harangi@geology.elte.hu (S. Harangi).

0377-0273/$ - see front matter
doi:10.1016/j.jvolgeores.2004.11.012

detected in the genesis of the Middle Ignimbrite Unit, based on the strong intra-sample geochemical variation both in the glasses and in the phenocrysts.

Keywords: LA-ICP-MS; ignimbrite; glass shard; silicic volcanism; tephrochronology; petrogenesis; Pannonian Basin

1. Introduction

Ash fall and pyroclastic flow deposits (e.g., ignimbrites) derived from eruption of silicic magmas often cover large areas and can extend for distances of several hundreds of kilometres. These volcanic products are formed during hours to weeks, i.e. during instantaneous geologic events, and consequently they provide unique chronological marker horizons in stratigraphic sections on a regional scale. Thorarinsson (1944, 1974), correlating the tephra horizons in Iceland, introduced the term tephrochronology, which has become an important field of Quaternary science (Westgate and Gorton, 1981; Sarna-Wojcicki et al., 1984, 1987; Bogaard and Schmincke, 1985; Froggatt and Lowe, 1990; Shane, 2000).

Pyroclastic deposits can, however, be subsequently easily eroded, broken apart and dispersed, making field studies difficult. Correlation of pyroclastic flow deposits (e.g., ignimbrites) could be particularly problematic due to additional effects such as vertical and horizontal zonation in physical and geochemical properties (Smith, 1960; Hildreth, 1981; Hildreth and Mahood, 1985). Hildreth and Mahood (1985) discussed a number of possible correlation tools for ash-flow tuffs and suggested that the composition of juvenile material and lithoclasts can be especially useful in addition to high-precision geochronological and paleomagnetic measurements. De Silva and Francis (1989) provided case studies for correlation of large ignimbrite sheets in the Central Andes and concluded that phenocryst chemistry (e.g. Fe, Mg, Mn and Ti content of biotite, hornblende and orthopyroxene) could be the most effective method for fingerprinting ignimbrite units. Shane et al. (2003) emphasized also the effectiveness of biotite composition in the correlation of Quaternary tephra beds. The major element composition of glass shards, which represents the liquid part of the erupted magma, has also been widely used to correlate Quaternary tephras (Froggatt, 1983, Stokes and Lowe, 1988, Shane and Froggatt, 1991, 1994; Stokes et al., 1992; Lowe et al., 1999). Trace element chemistry of glass shards is, however, a more powerful fingerprint of the erupted volcanic products, because trace elements show larger variability than the major elements. However, this method has not been widely used in tephrochronological studies, because of the laborious preparation procedure of separation of glass shards from the bulk rock (De Silva and Francis, 1989). In a review paper of tephrochronological studies in New Zealand, Shane (2000) concluded that grain-specific techniques such as laser-ablation inductively coupled plasma mass spectrometry (LA-ICP-MS) could become particularly important in the future.

The first application of LA-ICP-MS for tephrochronological purposes was conducted by Westgate et al. (1994), but they used separated multiple glass shard grains for analysis. More recently, the rapid development of this technique (Sylvester, 2001) has enabled the analysis of a large number of trace elements even in single glass shards in situ on a scale of 30–40 μm with very low (sub μg g^{-1}) detection limits (Pearce et al., 1999, 2002). This method allows the routine analysis of individual glass shards with minimal sample preparation, i.e. from standard thin sections (but with about 100 μm thickness) and meanwhile the petrographic characteristics of the sample can be also studied. The in situ trace element analysis of single glass shards provides additional benefits, such as checking the intra-sample chemical homogeneity and as a result providing an insight into the magma chamber processes and constraining the petrogenesis of silicic magmas (Bryant et al., 1999).

In this paper, we present a case study from the Northern Pannonian Basin, Eastern-Central Europe to show that in situ trace element data of glass shards from ignimbrites combined with mineral chemical data could be used effectively to correlate scattered silicic pyroclastic occurrences, with improved resolution over

existing palaeomagnetic and K–Ar geochronological techniques. In addition, these data can be used also to constrain the genesis of the silicic magmas.

2. Geological background

The Carpathian–Pannonian Region in Eastern Central Europe (Fig. 1) consists of an arcuate orogenic belt (the Carpathians) and an associated back-arc basin (the Pannonian Basin) formed as a part of the orogenic systems of the Alpine–Mediterranean region (Horváth and Berckhemer, 1982, Wortel and Spakman, 2000). Subduction of oceanic lithosphere of the Magura basin commenced in the Palaeogene and terminated gradually from west to east during the Middle Miocene to Quaternary (Royden and Burchfiel, 1982; Csontos et al., 1992; Tomek and Hall, 1993). The Pannonian Basin was formed by lithospheric extension during the Early to Middle Miocene due to the combined effect of collapse of overthickened crust and slab pull in the retreating subduction zone beneath the Outer Carpathians (Horváth, 1993; Fodor et al., 1999; Tari et al., 1999). The formation and tectonic evolution of this region were accompanied by widespread volcanic activity (Szabo et al., 1992; Seghedi et al., 1998; Harangi, 2001). Neogene volcanism started with explosive eruptions of silicic magmas in the Early Miocene (at about 21 Ma; Pécskay et al., 1995). This silicic volcanism lasted for about 7 Ma and can be divided into a pre-extensional and a syn-extensional stage. The latter one was contemporaneous with the early phase of the calc-alkaline andesitic to dacitic volcanism at the Northern Pannonian Basin. Calc-alkaline volcanic activity started at 16.5 Ma along the

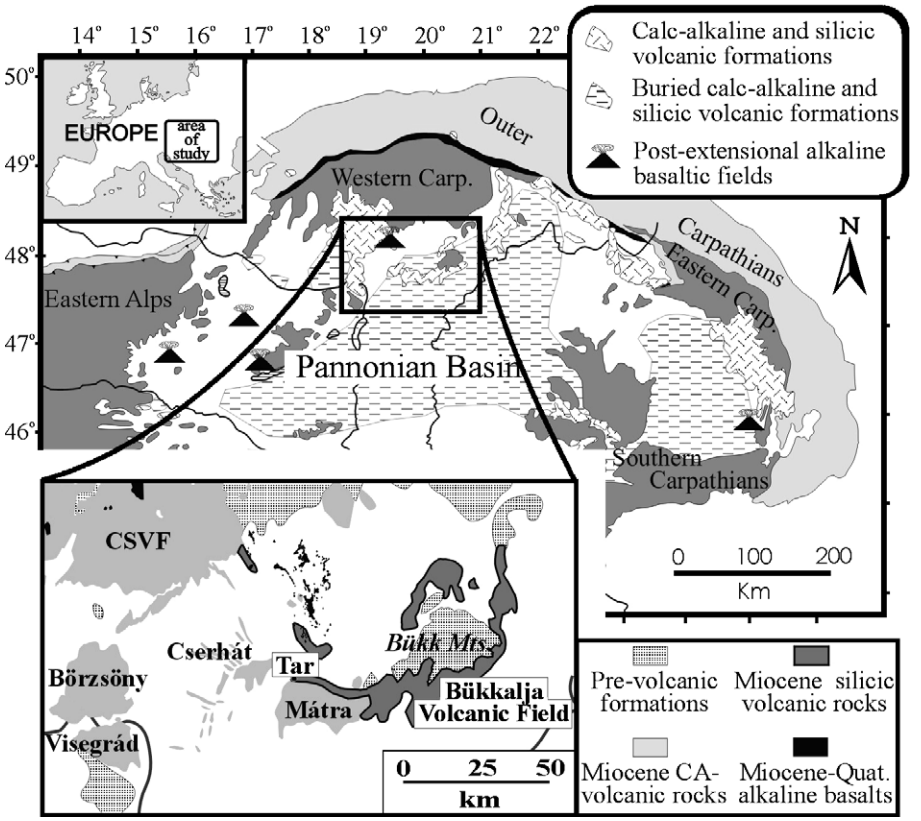

Fig. 1. Location of the study area in the Carpathian–Pannonian Region, Eastern-Central Europe. Carp—Carpathians, CSVF—Central Slovakian Volcanic Field.

Northern Pannonian Basin with eruption of garnet-bearing andesites and rhyodacites (Harangi et al., 2001) followed by mostly andesites and dacites during the next volcanic phases up to 9 Ma (Konečný et al., 1995; Harangi, 2001). In the eastern parts of the Carpathian–Pannonian Region, calc-alkaline volcanism started later, at about 14 Ma and shows a gradual younging towards the southeast with the final stages of magmatism occurring only at 13 ka (Mason et al., 1996, 1998). Eruptions of alkaline mafic rocks followed the calc-alkaline volcanism and they form monogenetic volcanic fields towards the inner parts of the Pannonian Basin (Embey-Isztin et al., 1993; Embey-Isztin and Dobosi, 1995).

The Miocene silicic volcanism resulted in rhyodacitic to high-Si rhyolitic volcanic products (predominantly ignimbrites and phreatomagmatic ash fall deposits; Pantó, 1963; Szakács et al., 1998) covering a large area in the Pannonian Basin. However, most of these rocks are buried by Late Miocene to Quaternary sediments (Fig. 1) due to strong post-rift subsidence. Outcrops of the silicic pyroclastic rocks are found mostly in the Northern Pannonian Basin, especially on the southern slopes of the uplifted Bükk Mts. (Bükkalja Volcanic Field, BVF; Figs. 1 and 2), where numerous scattered outcrops cover the whole sequence of the silicic volcanism from 21 Ma to 13.5 Ma (Márton and Pécskay, 1998; Szakács et al., 1998). Most of the exposed volcanic rocks are remarkably fresh, making this a key area to study the nature of the silicic pyroclastic units. However, correlation of the pyroclastic rocks derived from the same volcanic eruption phase is very difficult even in this area where the rocks are well exposed, due to the lack of direct contact between units and with fossiliferous sedimentary beds, the very similar macroscopic features in the field, and the insufficient accuracy and precision of existing K–

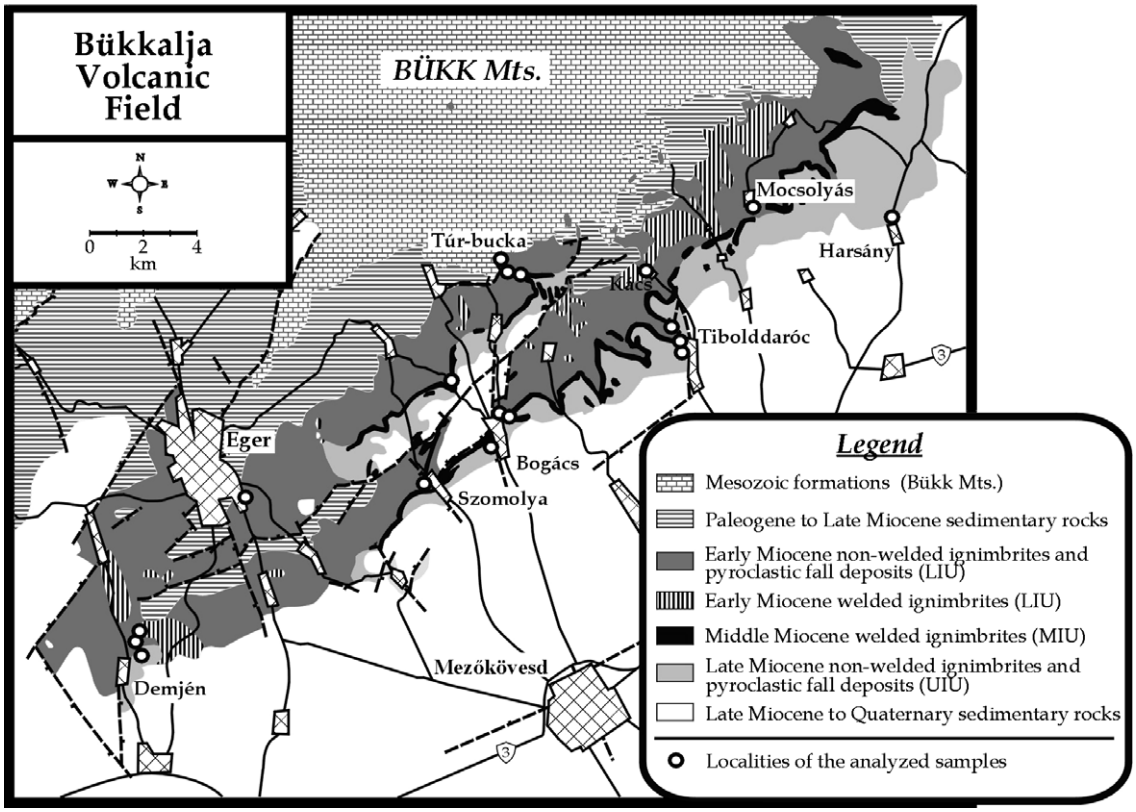

Fig. 2. Simplified geological map of the Bükkalja Volcanic Field showing the areal distribution of the main ignimbrite units (modified from Szakács et al., 1998) and the localities of the analyzed samples.

Ar age data (Márton and Pécskay, 1998). Nevertheless, three main units were distinguished based on paleomagnetic data, because two major rotation events occurred in this area during the Miocene (Márton and Fodor, 1995; Márton and Pécskay, 1998). This subdivision (Lower, Middle and Upper Ignimbrite Units; LIU, MIU and UIU, respectively; Fig. 2) can serve as a starting point in the correlation of the pyroclastic sequence.

3. Volcanology and petrology

The Miocene volcanic rocks in the BVF cover a surface area of approximately 300 km^2, with a continuation at depth towards the south. The volcanic sequence reaches up to 750 m in thickness, based upon borehole data (Szakács et al., 1998). Most of the volcanic rocks are pyroclastic flow deposits (ignimbrites with minor scoria-flows) with both non-welded and welded facies (Varga, 1981; Capaccioni et al., 1995; Szakács et al., 1998). In addition, phreatomagmatic pyroclastic fall layers can be found throughout the area as accretionary lapilli-bearing tuffs. No lava flows associated with the silicic pyroclastic suite have been identified in this area.

The most common volcanic lithofacies is the non-welded pumiceous pyroclastic flow deposit (ignimbrite), which is the dominant rock type of the LIU and UIU. They are poorly sorted block-bearing lapilli tuffs (Fig. 3A and B). The maximum size of the pumices can reach 40–50 cm. The pumices are phenocryst poor (generally <5%), consisting of quartz, plagioclase, biotite and occasional sanidine or hornblende. Zircon, ilmenite and allanite occur as accessory mineral phases with variable amounts. The lithoclasts (5–10%) have dominantly igneous origin (basaltic andesite, andesite and rhyolite). Most of the lithoclasts are porphyritic, containing plagioclase and orthopyroxene phenocrysts with minor amounts of clinopyroxene, hornblende, biotite or quartz, sitting in a glassy groundmass. The matrix of the non-welded ignimbrites is composed of cuspate, pumiceous to platy glass shards and loose crystals (Fig. 3E) with a similar mineral assemblage to the pumices. This lithofacies shows very similar volcanological character both in the LIU and UIU, making it difficult to distinguish the flow units in the field.

Variably welded pyroclastic flow deposits occur both in the LIU and MIU. The welded ignimbrite of the MIU appears to follow a southwest to northeast trending narrow belt in the BVF, whereas that of the LIU can be found in scattered localities (Fig. 2). No contacts between the non-welded and welded ignimbrites have been found in the field. The welded pyroclastic rocks are fiamme-bearing lapilli tuffs (Fig. 3C and D) with a range of colours (grey, brown and red) and varying sizes of fiamme (few millimeters to 20 cm in length). The fiamme consist of a fresh glassy groundmass occasionally with visible structural remnants of the original pumices and glass shards. In some localities, flattened glass shards can be still observed in the matrix (Fig. 3F). Some of the fiamme show incipient perlitic structure. The quantity of phenocrysts in the fiamme is strongly variable from a few percent in the LIU to 50% in the MIU. The two welded pyroclastic units also differ in their mineralogy. Although quartz, plagioclase and biotite are common in both units, orthopyroxene is found only in the MIU rocks. Ilmenite and allanite are characteristic accessory mineral phases in the MIU, whereas zircon is more frequent in the LIU rocks. The matrix contains similar mineral assemblage as the fiamme.

In addition to the dominant ignimbrite deposits, a scoria-flow deposit occurs also in the MIU overlying the fiamme-bearing pyroclastic beds. It contains a mixed juvenile clast population with dark scoria fragments, pumices and composite clasts (Czuppon et al., 2001; Harangi et al., 2002). Segregation pipes are commonly observed in this deposit. Accretionary lapilli-bearing tuffs are also occasionally found in the BVF. They are crystal-poor vitric tuffs containing cuspate and platy glass shards and loose phenocrysts of quartz, plagioclase and biotite with rare hornblende.

4. Analytical techniques

The major element composition of the glasses (glass shards, pumices and fiamme) and the main mineral phases were determined using a CAMECA SX100 electron microprobe with a 15 kV voltage and a 20 nA beam current at the Institute of Petrology, University of Vienna, Austria. Further analysis was carried out using a JEOL-733 Superprobe equipped

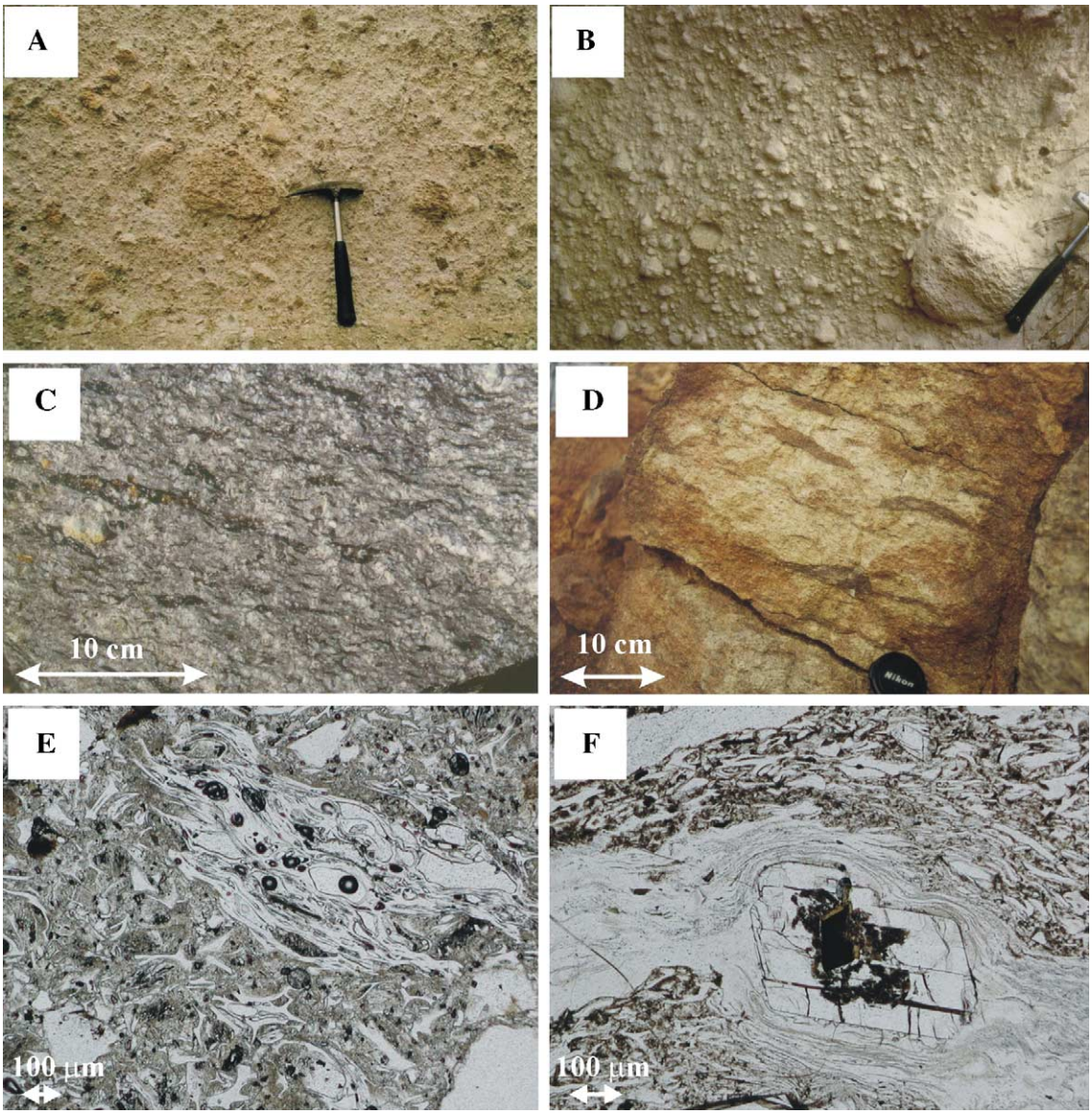

Fig. 3. Volcanological and petrographical characters of the ignimbrites of the Bükkalja Volcanic Field. (A) Non-welded ignimbrite at Szomolya (LIU); (B) non-welded ignimbrite at Tibolddaróc (UIU); (C) fiamme-bearing, partially welded ignimbrite at Pünkösdhegy, Demjén (LIU); (D) fiamme-bearing welded ignimbrite at Vén-hegy, Bogács (MIU); (E) typical microscopic texture of the unwelded ignimbrites (Mocsolyás, LIU); (F) typical microscopic texture of the partially welded ignimbrites (Túr-bucka, LIU). LA-ICP-MS analyses were carried out on single glass shards and on the glasses of fiamme.

with an Oxford Instrument ISIS energy dispersive system (Birkbeck College, University of London) with a 15 kV accelerating voltage for 100 s. Data from both laboratories were checked by analyzing the same samples and the results were within 1–5% of each other. During glass analysis we used a defocused beam (5 μm) to minimise the alkali loss.

We determined 25 trace elements in 221 glass shards and fiamme from 25 samples of different localities of the BVF by LA-ICP-MS using a 193 nm

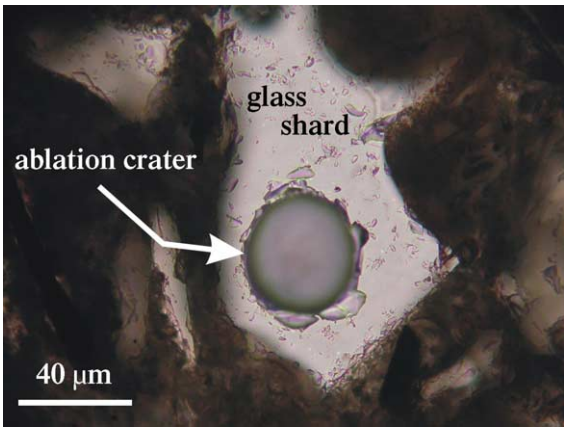

Fig. 4. Ablation crater with a width of 40 μm in a single glass shard (Harsány, UIU).

ArF excimer laser ablation system (MicroLas GeoLas 200Q) in combination with a quadrupole ICP-MS (Micromass Platform ICP) at Utrecht University (Mason and Kraan, 2002). Polished thin sections with about 100 μm thickness were used for analysis. Glass shards were identified with a Zeiss petrographic microscope attached to the LA-ICP-MS instrument. Ablation was performed at a fixed point on the sample with an irradiance of 0.2 GW cm^{-2}, a laser pulse repetition rate of 10 Hz and an ablation crater diameter of 40 μm (Fig. 4). The signal recorded by the ICP-MS during ablation was carefully checked for inclusions and compositional boundaries to ensure that only data for the glass shards were integrated (Fig. 5). Quantitative concentrations were calculated using NIST SRM 612 as a calibration standard (Pearce et al., 1997) with Ca (previously determined by electron microprobe analysis) as an internal standard element. The USGS reference glass BCR-2G was continuously measured throughout the analysis of the glasses and the results were within 5–10% of recommended values. Detection limits were typically in the range 0.01–1 μg g^{-1} and internal precision was <5% RSD (1σ) for concentrations above 1 μg g^{-1} and <15% RSD (1σ) below 1 μg g^{-1}.

5. Geochemistry

5.1. Major element composition of glasses and the main minerals

The major element compositions of the glasses and the main mineral phases of representative samples are presented in Tables 1 and 2. The glasses (glass shards, pumices and fiamme) of the BVF pyroclastic rocks are remarkably fresh based on the microscopic

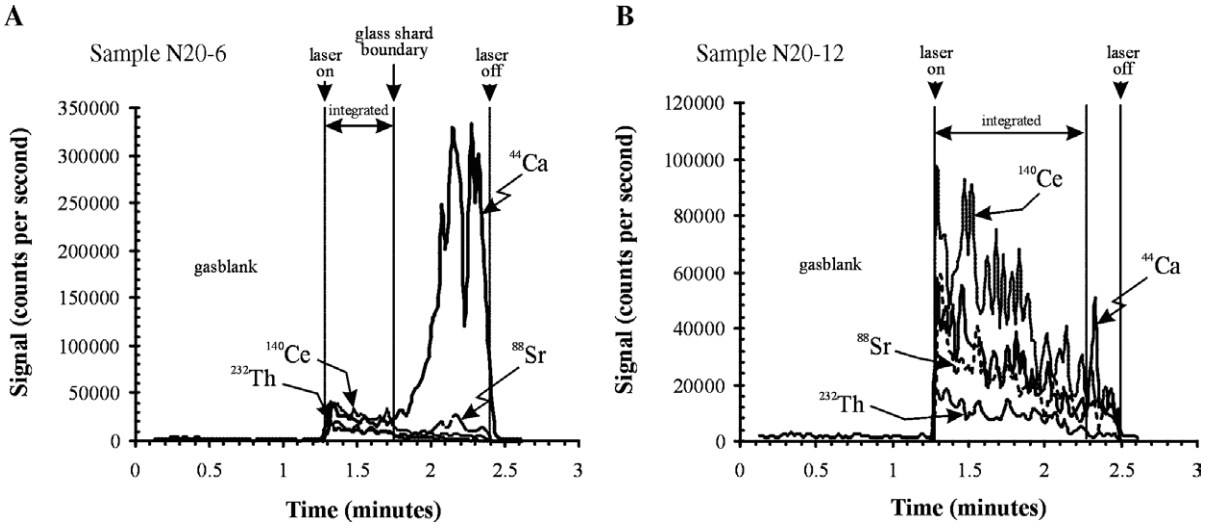

Fig. 5. Time-resolved signals for selected isotopes during LA-ICP-MS analysis of two glass shards with different thickness (sample N20; Harsány, UIU). Note the sharp change in the signal at the grain boundary. For calculation the concentration of trace elements, only the signals coming from the glass shard were integrated.

Table 1
Major (in wt.%) and trace element (in ppm) concentrations of glasses from representative samples of the Bükkalja Volcanic Field

Unit	LIU						MIU					UIU-W		UIU-E			Tar, NW-Mátra	
Sample	U13L-4-2	BKA10-5	N1-1-2	N37-1	N14-12	N25-2	U15L-4	V1-4-1	V1-26	V1-5	V1-8	N13-2	BKA17-1	TD2-9	TD2-6-2	N20-2-1	TAR-11	TAR-12
Glass type	gs	gs	fi	gs	gs	gs	fi	fi	fi	gs	gs	gs	gs	gs	gs	gs	gs	gs
Locality	Kács	Túr-bucka	Túr-bucka	Szomolya	Demjén	Mocsolyás	Tibolddaróc	Bogács, Vén-hill	Bogács, Vén-hill	Bogács, Vén-hill	Bogács, Vén-hill	Demjén	Bogács	Tibolddaróc	Tibolddaróc	Harsány	Tar	Tar
SiO_2	77.05	77.30	77.05	77.23	78.03	77.31	71.88	76.01	76.55	75.29	77.44	77.73	77.88	78.41	77.71	77.24	77.50	77.38
TiO_2	0.07	n.d.	n.d.	0.12	n.d.	n.d.	0.39	0.09	0.11	0.18	n.d.	0.06	0.06	0.04	0.04	0.06	0.09	0.07
Al_2O_3	12.77	12.94	13.37	12.86	12.69	13.20	15.59	13.99	13.54	13.98	12.79	12.69	12.62	12.90	12.87	12.99	12.90	12.74
FeO^t	1.00	0.67	0.43	1.40	0.64	0.46	1.79	0.51	0.61	0.54	0.35	0.27	1.08	0.84	0.84	0.71	1.19	1.13
MgO	0.10	n.d.	n.d.	0.11	0.06	0.06	0.58	n.d.	0.06	n.d.	n.d.	n.d.	0.06	n.d.	0.05	0.06	0.09	0.10
CaO	1.00	0.70	0.64	1.27	0.94	0.95	1.93	0.95	0.94	1.35	0.03	0.87	1.05	0.62	0.63	0.65	1.09	1.15
Na_2O	2.45	2.48	2.70	2.28	2.01	2.91	1.72	2.01	2.12	2.06	1.63	2.12	1.89	2.78	2.42	3.70	2.26	2.10
K_2O	5.55	5.91	5.81	4.74	5.63	5.10	6.12	6.45	6.08	6.60	7.75	6.27	5.36	4.41	5.45	4.60	4.88	5.33
LOI*	4.36	3.97	4.61	4.95	4.98	4.35	4.69	5.85	5.38	5.32	5.08	5.04	6.82	5.18	4.91	3.93	4.44	4.43
Rb	152	180	186	216	153	151	181	320	378	185	364	133	200	179	205	162	164	178
Sr	67	68	66	87	90	69	181	67	67	113	9	66	84	31	34	36	83	88
Y	14.6	17.8	17.4	22.3	18.2	16.5	40.2	35.6	35.1	26.3	38.6	6.6	8.2	39.7	38.4	31.6	8.7	9.1
Zr	51	60	54	70	75	52	373	179	127	141	63	57	63	66	92	65	74	86
Nb	7.8	8.4	8.5	11.4	9.2	9.1	12.7	16.7	16.2	10.9	13.3	6.1	6.9	14.0	16.8	11.6	6.6	6.9
Ba	744	789	752	912	741	610	1074	1252	1085	794	461	510	715	723	705	716	523	585
La	20.8	24.8	18.2	25.5	27.6	21.2	50.2	71.6	57.7	53.8	22.0	21.0	26.4	21.6	22.7	20.1	19.9	24.0
Ce	42.0	49.9	37.4	47.9	51.2	39.8	94.8	140.9	124.9	95.8	50.1	32.3	41.9	46.1	49.3	38.3	34.3	37.7
Pr	4.00	4.80	3.60	5.30	5.17	4.00	10.92	13.47	12.00	10.58	5.90	3.09	3.58	4.90	5.35	4.78	3.08	3.19
Nd	13.10	15.50	12.40	16.80	18.70	14.80	39.72	47.60	43.88	34.95	25.30	8.64	9.95	19.37	22.27	16.68	10.01	10.67
Sm	3.40	3.35	2.55	3.95	3.41	2.80	8.16	8.80	9.35	6.41	7.30	1.33	1.29	4.84	5.15	4.43	1.65	1.65
Eu	0.38	0.50	0.37	0.57	0.44	0.53	1.56	0.92	0.68	0.98	0.20	0.20	0.29	0.34	0.33	0.37	0.31	0.31
Gd	2.70	2.70	1.50	3.60	3.19	3.10	8.04	8.40	9.66	6.38	7.35	1.60	1.34	5.95	5.09	5.48	1.54	1.65
Dy	2.50	3.00	2.90	3.30	2.97	2.50	7.02	7.20	7.51	4.28	7.73	1.12	1.34	5.95	6.49	5.60	1.43	1.54
Er	1.45	1.85	1.45	2.10	1.87	1.55	4.14	3.67	3.82	2.44	4.45	0.72	0.84	3.97	3.82	3.44	0.80	0.88
Yb	1.80	1.85	2.05	2.60	1.93	1.75	4.50	3.60	3.85	3.00	4.50	0.91	0.73	4.08	4.14	3.50	0.91	1.32
Lu	0.25	0.30	0.27	0.36	0.31	0.23	0.72	0.48	0.49	0.37	0.70	0.18	0.22	0.61	0.64	0.49	0.23	0.24
Hf	2.20	2.60	1.80	2.80	2.53	2.10	8.52	5.33	5.17	4.35	4.60	1.81	2.24	3.27	2.93	2.57	2.64	2.31
Ta	0.90	1.10	1.18	1.50	0.81	1.10	0.96	1.28	1.42	0.98	2.30	0.81	1.01	1.63	1.53	1.27	0.75	0.85
Pb	26.6	33.6	28.6	34.2	27.6	25.9	28.1	26.8	25.4	12.6	11.8	22.6	31.5	24.5	25.8	21.7	31.5	31.7
Th	15.9	17.8	16.4	21.0	17.6	16.8	17.5	23.5	24.1	21.3	20.6	17.3	22.5	15.4	15.4	13.2	17.4	21.1
U	5.30	5.60	6.10	7.70	7.59	4.40	4.44	5.47	7.20	5.25	7.05	5.23	5.81	5.72	5.22	4.20	6.49	6.71

Major elements were determined by microprobe and were recalculated to 100% on anhydrous basis. LOI* denoted the difference of the measured total from 100%. The trace elements were determined by laser ablation ICP-MS. LIU—lower ignimbrite unit; MIU—middle ignimbrite unit; UIU—upper ignimbrite unit (W—west; E—east); gs—glass shard; fi—fiamme. The localities are shown in Figs. 1 and 2.

Table 2
Representative electron microprobe analyses of biotites and plagioclases of the Miocene ignimbrites of the Bükkalja Volcanic Field (for abbreviations see Table 1)

Biotites

Unit	LIU			MIU			UIU-E			UIU-W
Locality	Demjén	Túr-bucka	Mészhegy	Vénhegy, Bogács	Vénhegy, Bogács	Tibold-daróc	Harsány	Tibold-daróc	Harsány	Demjén
SiO_2	36.31	36.12	36.4	34.78	34.65	35.32	34.49	34.39	34.43	34.5
TiO_2	3.45	3.39	3.56	4.29	4.6	4.7	3.61	3.89	3.66	4.73
Al_2O_3	14.37	13.99	13.8	13.93	14.35	13.69	13.23	13.85	13.46	13.7
FeO	23.71	24.08	22.84	27.89	26.37	24.51	28.64	29.33	28.6	22.84
MgO	0.23	0.19	0.27	0.27	0.16	0.16	0.38	0.25	0.4	0.24
CaO	9.37	9.3	9.07	4.76	6.97	8.68	5.65	4.89	5.75	9.5
Na_2O	0.42	0.54	1.06	1.07	0.57	0.64	0.51	0.39	0.45	0.42
K_2O	8.51	8.65	8.58	8.63	8.62	8.52	8.56	8.56	8.71	8.64
TOTAL:	96.37	96.26	95.58	95.62	96.29	96.22	95.07	95.55	95.46	94.57

Plagioclases

Unit	LIU				MIU				UIU-W		UIU-E		
Locality	Szomolya	Túr-bucka	Mészhegy	Demjén	Vénhegy, Bogács	Vénhegy, Bogács	Vénhegy, Bogács	Vénhegy, Bogács	Demjén	Demjén	Harsány	Harsány	Tibold-daróc
SiO_2	56.72	58.48	55.17	56.80	53.50	50.59	57.00	46.30	53.23	57.12	63.44	58.35	63.69
Al_2O_3	27.22	26.36	28.86	27.46	29.22	30.81	26.89	33.83	29.87	27.96	23.25	26.20	23.50
FeO	0.18	0.12	0.07	0.12	0.18	0.21	0.20	0.30	0.37	0.24	0.14	0.14	0.05
CaO	9.95	8.61	10.31	9.68	12.24	14.29	9.40	17.73	12.60	9.09	4.74	8.41	3.40
Na_2O	5.49	6.65	4.73	6.06	4.30	3.28	5.71	1.39	4.52	5.90	6.92	6.38	7.76
K_2O	0.35	0.41	0.35	0.38	0.25	0.16	0.36	0.04	0.21	0.54	0.87	0.40	1.13
TOTAL:	99.90	100.63	99.49	100.50	99.69	99.34	99.56	99.59	100.80	100.85	99.36	99.88	99.53
An	49.02	40.75	53.46	45.88	60.24	70.00	46.63	87.37	59.93	44.54	25.88	41.16	18.10
Ab	48.92	56.95	44.38	51.98	38.30	29.07	51.25	12.40	38.89	52.32	68.47	56.51	74.75
Or	2.06	2.30	2.16	2.14	1.46	0.93	2.12	0.23	1.18	3.14	5.65	2.33	7.15

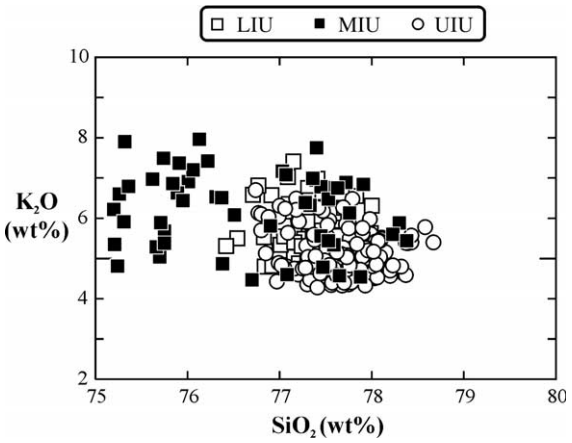

Fig. 6. SiO_2 vs. K_2O diagram showing major element compositional variation of the glasses of the Bükkalja ignimbrites. Note the overlap of the LIU and UIU glasses.

observations in spite of the relatively old ages (13.5–21 Ma) of the deposits. The LOI content of the glasses, calculated from the deficiency in the total of the microprobe analysis from 100%, is mainly in the range between 3 and 6 wt.% irrespective of their types (glass shard, pumice or fiamme glass). In the interpretation of the major element data of glasses, we recalculated them to 100% on anhydrous basis. The glasses have a relatively homogeneous, rhyolitic major element character and are strongly potassic (Fig. 6; SiO_2=75–78.5 wt.%, K_2O=4–8 wt.%, K_2O/Na_2O=1.5–5). Glasses from the LIU and UIU are indistinguishable based on their major elements, whereas the MIU glasses have usually less SiO_2 and slightly higher K_2O/Na_2O ratio.

Plagioclases and biotites are common minerals in each pyroclastic unit of the BVF. Most of the plagioclase crystals are fairly homogeneous, while the others show normal or occasional reverse zoning. They show a wide range of composition from An_{18} to An_{90} (Fig. 7). This large compositional variation characterizes especially the plagioclases of the MIU ($An_{22–90}$), whereas those of the LIU and UIU show more restricted anorthite content ($An_{28–58}$ and $An_{20–60}$, respectively). Biotites are also ubiquitous, although some of them are altered. The MgO content of the fresh biotites is in the range between 4.5 and 9 wt.%, whereas the TiO_2 content varies between 3 to 5 wt.% (Fig. 6). The largest and most continuous compositional variation is found, as for plagioclase, in the MIU. The biotites of the LIU have fairly uniform chemistry (MgO=8.5–9.5 wt.%, TiO_2=3.2–3.8 wt.%), whereas those of the UIU appear to show a bimodal composition. Biotites from the UIU ignimbrites occurring at the eastern part of the Bükkalja Volcanic Field, have characteristically low MgO (5.3–6 wt.%) and low TiO_2 (3.4–3.7 wt.%), whereas biotites from the western part of the Bükkalja have typically higher MgO (8.8–

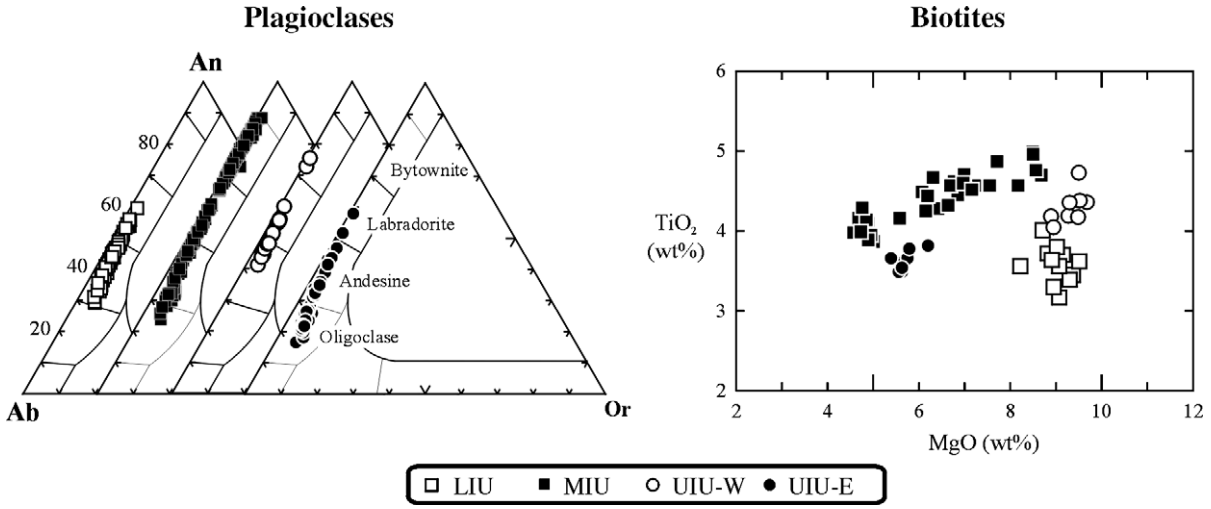

Fig. 7. Compositional variation of plagioclases and biotites from different ignimbrite units of the BVF. The UIU is divided into two groups, a western and an eastern one (UIU-W and UIU-E, respectively) based on the difference in the mineral chemical data.

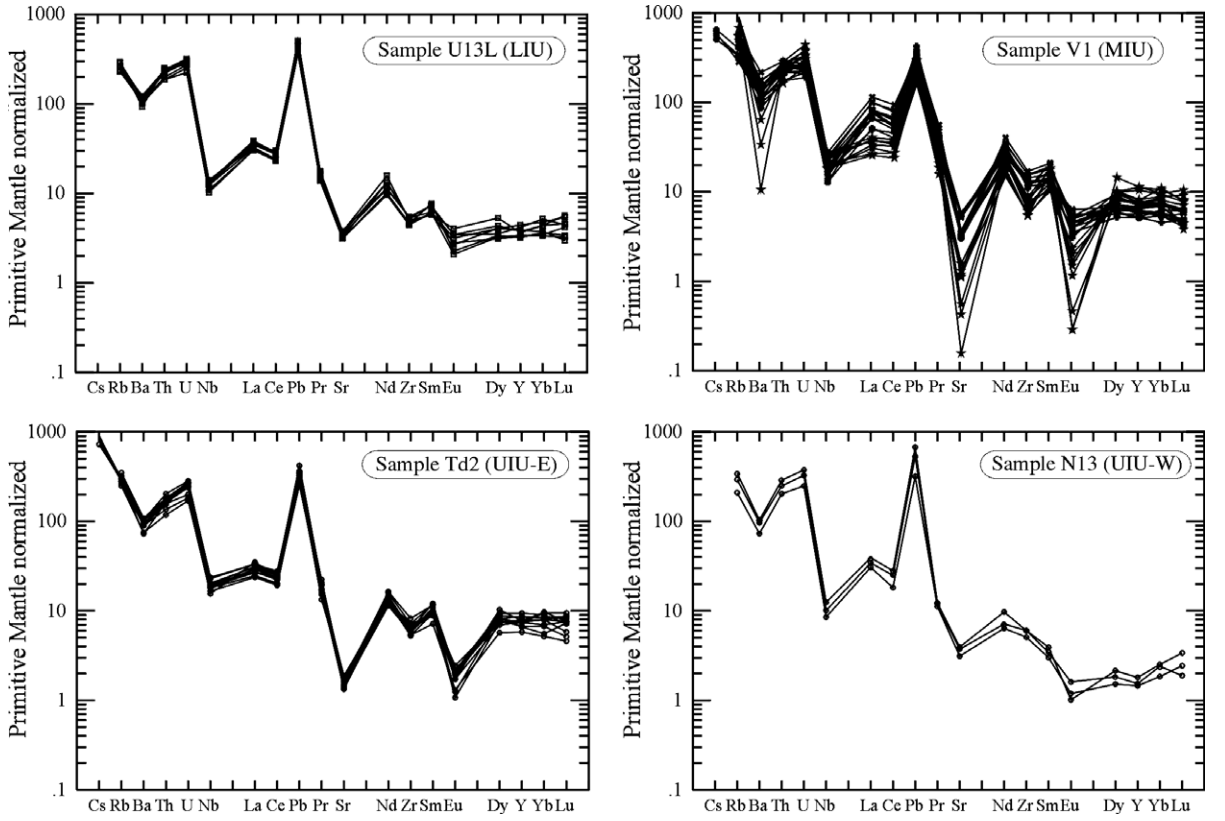

Fig. 8. Primitive mantle (Sun and McDonough, 1989) normalized trace element patterns of glasses from single samples (U13L: Kács; V1: Vén-hegy, Bogács; Td2: Tibolddaróc; N13: Demjén). Note the relatively homogeneous character of the LIU and UIU samples, but the strong compositional heterogeneity of glasses in the sample V1.

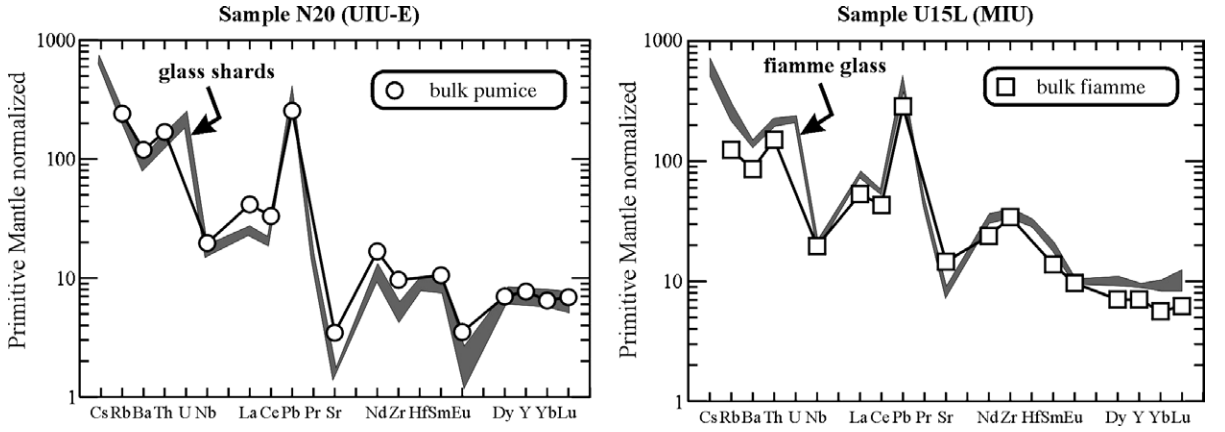

Fig. 9. Comparison of primitive mantle (Sun and McDonough, 1989) normalized trace element patterns of glasses and bulk pumice/fiamme from the same sample.

9.8 wt.%) and higher TiO_2 (4–4.7 wt.%). Orthopyroxenes are confined to the pyroclastic deposits in the MIU. Both homogeneous and normally zoned crystals occur and have the composition of ferroan enstatite ($En_{49–82}$ and $Wo_{1–3}$).

5.2. Trace element composition of glasses

Results of the LA-ICP-MS trace element analyses of representative samples are given in Table 1. Each analysis was inspected individually, based on the

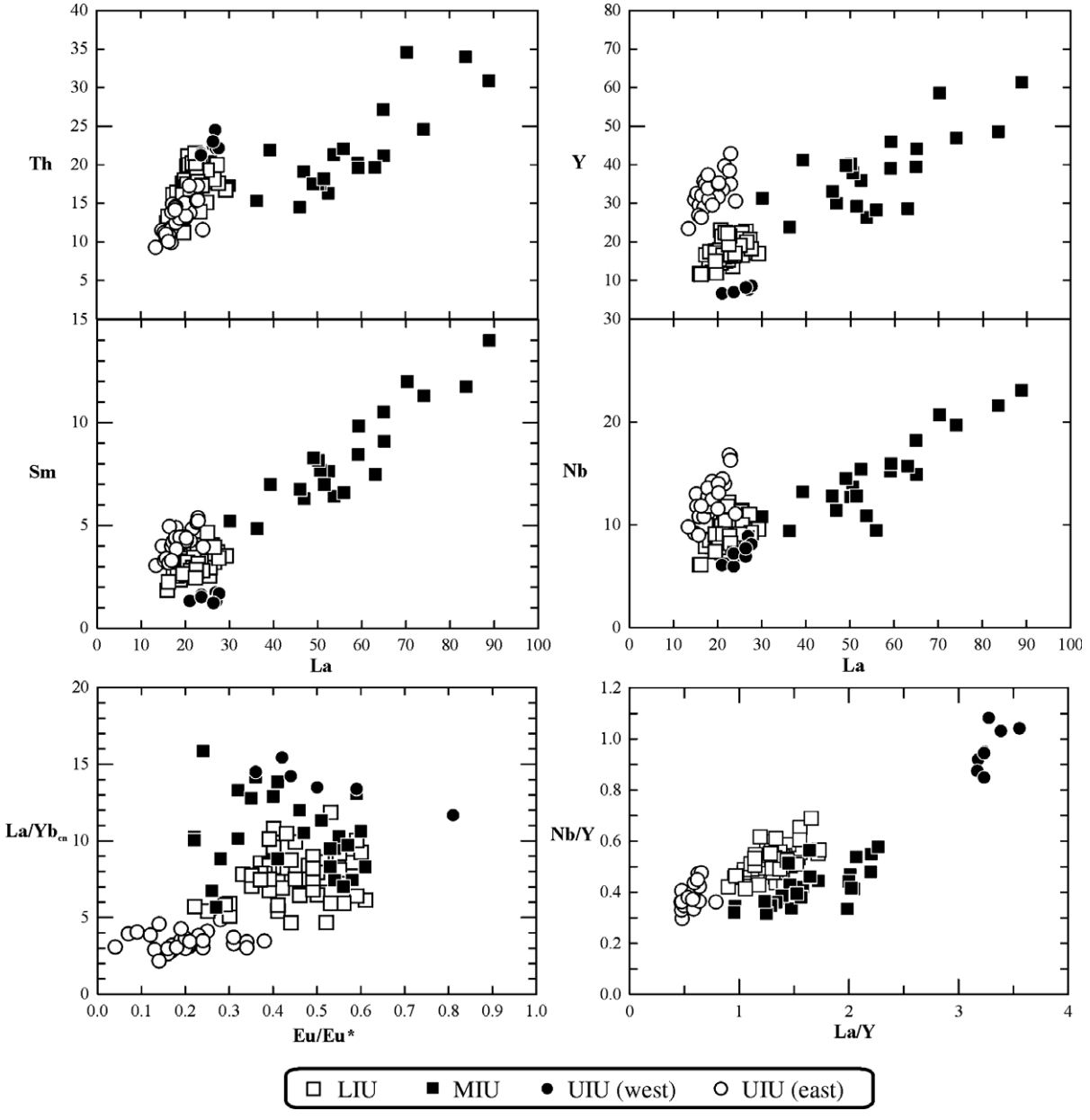

Fig. 10. Variation of incompatible trace elements and trace element ratios of glasses. Note the separation of main ignimbrite units in these diagrams. Symbols as in Fig. 7.

time-resolved signals of several elements (Fig. 5) to remove any spurious data derived either from a microcryst or from the matrix surrounding the glass shard. The analyzed glasses do not show significant geochemical variation in single samples of the LIU and UIU (Fig. 8). However, there is great compositional heterogeneity within and between single samples derived from the MIU (Fig. 8). For example, glasses in the sample V1 show considerable variation in Ba, Sr, Zr and rare earth element (REE) contents. In contrast, no compositional differences can be found between the glass shards and the fiamme in the partially welded (i.e. where the glass shards are still visible, although they are flattened; Fig. 3F) ignimbrite samples of the LIU. No significant differences in composition were observed between the glass shards and the bulk pumice blocks, or between the fiamme glass and the bulk fiamme in the same sample (Fig. 9). Bulk pumices have a slightly higher Sr, Ba, Eu, Zr and light REE content than the glass shards, reflecting their enclosed phenocrysts and accessory mineral assemblage (plagioclase, biotite, zircon). Pearce et al. (2002) observed the same difference in the trace element contents of bulk pumices and single glass shards in the Minoan tephra layers. The bulk fiamme contains slightly lower concentrations of incompatible elements than the fiamme glass, a feature that can be explained by the abundant orthopyroxene (it is relatively poor in most trace elements) in the fiamme.

The primitive mantle normalized trace element patterns of the glasses (Fig. 8), show, in general, a strong enrichment in the large ion lithophile elements (LILE; e.g., Cs, Rb, Ba) and Pb, as well as in Th and U, whereas they are relatively depleted in Nb, Sr and Eu. However, the magnitude of positive and negative anomalies and the total concentration of the incompatible trace elements show a systematic variation. The highest incompatible trace element content is shown by the fiamme of the MIU samples (Fig. 8). It is remarkable that glasses of the pyroclastic rocks of the UIU occurring at the western and eastern parts of the BVF are distinct in their trace element compositions (Fig. 10). The samples from the western parts show only a small negative Eu-anomaly (Eu/Eu*=0.4–0.65) and a strong depletion in the heavy REE, whereas those from the eastern part have a strong negative Eu-anomaly (Eu/Eu*=0.2–0.4) and relatively minor light REE/heavy REE fractionation ($[La/Yb]_{cn}$=3.5 on average, whereas it is 13 to 15 in the UIU samples at the western BVF; Fig. 10). Trace element characteristics of the LIU glasses lie between these two end-member types (Eu/Eu*=0.3–0.6, $[La/Yb]_{cn}$=6.5 to 10).

6. Discussion

6.1. Correlation of pyroclastic units

The composition of juvenile components (phenocrysts and glasses) in pyroclastic deposits reflects the chemistry of the erupted magma. A change in the composition of the magma erupted in different episodes of the silicic volcanism should thus be reflected in the chemistry of the phenocrysts and the glasses. Indeed, the modal composition of the phenocrysts (occurrence and lack of certain minerals, as well as change in the relative amounts of them) and the chemical variability of plagioclases and biotites (Fig. 7) appear to be a possible correlation tool in the Bükkalja Volcanic Field. However, the best candidate to characterize the erupting magma is the quenched fragment of the liquid part of the magma, i.e. the glass shards. Pyroclastic eruptive units can thus be correlated by determining the composition of the glasses (Westgate and Gorton, 1981; Sarna-Wojcicki et al., 1984; Westgate et al., 1994, 1998; Pearce et al., 1999, 2002), providing that alteration, compositional zonation and mixing are taken into account (Hildreth and Mahood, 1985).

6.1.1. Correlation by petrography and mineral chemistry

The modal composition of the phenocrysts provides a possible tool to distinguish the partially to densely welded ignimbrites in this area. Orthopyroxene can be found only in the fiamme-bearing ignimbrites of the MIU, while it is lacking in the welded ignimbrites of the LIU. Amphibole (hornblende) is present also in the pyroclastic rocks of the MIU, but appears in some non-welded ignimbrites (UIU at the western parts of the Bükkalja Volcanic Field, denoted UIU-W), too. Among the feldspars, plagioclase is the dominant mineral throughout the whole volcanic sequence, but occasionally sanidine can be also found, mostly in the non-welded

ignimbrites of the UIU at the eastern part of the Bükkalja (denoted UIU-E). Thus, a rough distinction can be made using the phenocryst assemblage, although the accuracy of this method is limited.

Plagioclase and biotite occur in each pyroclastic deposit and they show wide variation in composition (Fig. 7). Biotites, however, show often incipient to strong alteration that makes the interpretation of the microprobe data difficult and a limitation of the use of this mineral. Composition of plagioclases varies from An=18 to 90 mol% and shows some systematic differences (Fig. 7). Plagioclases from the MIU ignimbrites have a very wide compositional range ($An_{25–90}$), whereas they show more restricted ranges in the samples of the LIU and UIU. Although they overlap each other in the andesine field ($An_{30–50}$), plagioclases in the UIU-E pyroclastic rocks often show a more sodic composition ($An_{18–30}$), whereas they shift towards the more calcic end-member in the UIU-W samples. The most unambiguous result in distinguishing pyroclastic units in this region can be obtained using the composition of fresh biotites (Fig. 7). De Silva and Francis (1989) and Chesner (1998) could also successfully use the microprobe determination of Fe, Mg, Ti and Mn for biotite to discriminate ignimbrite units in the Central Andes and within the Toba Tuffs, Indonesia, respectively. The biotites in the Bükkalja ignimbrites are usually more iron-rich (FeO^{tot}=22–31 wt.%) than those in the ignimbrites of the Andes and in the Toba Tuffs. In the MgO vs. TiO_2 diagram, the three pyroclastic units distinguished by palaeomagnetic data (i.e., LIU, MIU and UIU) are clearly separated from each other. Furthermore, the UIU can be subdivided into two groups, i.e. the non-welded ignimbrites at the western and eastern parts of the Bükkalja Volcanic Field (UIU-W and UIU-E). It is remarkable that the MIU biotites show a wide range in FeO and MgO contents, similarly to the wide range of An-content of plagioclases in these rocks. On the contrary, biotites of the other three ignimbrites units show fairly homogeneous, but distinct, composition.

In summary, the petrographic features (i.e., occurrence or lack of certain minerals) and the composition of the phenocrysts phases, especially that of biotites, can be applied as correlation tools for the Bükkalja ignimbrites. However, obtaining sufficient amount of data (e.g., avoiding altered biotites) can be time consuming.

6.1.2. Correlation by glass chemistry

The glasses (glass shards, pumice and fiamme glass) of the Bükkalja ignimbrites are usually fresh, i.e. they do not show post-eruptive recrystallization. Therefore, their composition still reflects the chemistry of the liquid part of the erupted magma. Most of the glasses are high-Si potassic rhyolite (SiO_2>75 wt.%, K_2O>4 wt.%; recalculated to 100%, on anhydrous basis), whereas the MIU contains dacitic glasses, too. Unfortunately, the major element composition of the glasses is very similar (Fig. 6), thus these data cannot be used to distinguish the pyroclastic units in Bükkalja. Trace elements are usually decoupled from the major elements and show greater and more discriminative variation in volcanic glasses (Sarna-Wojcicki et al., 1984; De Silva and Francis, 1989; Westgate et al., 1998; Clift and Blusztajn, 1999; Shane, 2000). The grain-specific LA-ICP-MS technique enables the rapid analysis of single glass shards from thin sections and provides more reliable trace element data for glasses than other techniques which use bulk glass separates for analysis (Pearce et al., 1999, 2002).

However, first the results have to be checked as to whether the final data are derived exclusively from the glass or the laser penetrated microcrysts or any material beneath the glass shard. The signals recorded by the ICP-MS during ablation can indicate these contaminations sensitively (Günther, 2001). The Fig. 5A shows an example, when only a very thin glass shard was analyzed. After approximately 30 seconds, the signal of ^{44}Ca and ^{88}Sr isotopes increased, implying the presence of feldspar beneath the glass shard. Nevertheless, integration of only the early range of data could give still reliable result for the trace element composition of the glass shard. The Fig. 5B presents another example from the same sample, where signals were coming entirely from the glass during almost the whole counting time.

Glasses of the Bükkalja ignimbrites show characteristic trace element fingerprints for each units (Figs. 8 and 10). The discriminator elements are Nb, Y, Sm, Eu and the heavy REE, whereas the MIU samples are characterized by distinctively high concentration of light REE. The degree of the negative Eu-anomaly, as expressed by Eu/Eu*, shows also systematic variation. The UIU-E glasses have the most pronounced negative Eu-anomaly (Eu/Eu*<0.4). Combining these

elements, an effective discrimination between the main pyroclastic units of Bükkalja can be achieved based on the La/Y, Nb/Y, La/Nb and Th/Nb ratios (Figs. 10 and 12). Using these geochemical parameters, pyroclastic rocks from scattered outcrops can be readily correlated over distances of several tens of km. The trace element fingerprints of individual glasses support also the distinction of two units within the UIU as was suggested also by the chemistry of biotites. Thus, a more refined correlation could be obtained using geochemical characteristics of the juvenile components of the ignimbrites than using geochronological and palaeomagnetic data. Based on the trace element characteristics of the glasses, we could refine the areal distribution of the silicic pyroclastic units in the BVF (Fig. 2), slightly modifying the previous geological maps of this region (Szakács et al., 1998).

In Fig. 11, we present an example of how this geochemical correlation can be extended over larger distances from the BVF. Approximately 40 km west from the outcrops of the UIU-W pyroclastic rocks, a thick non-welded ignimbrite can be found NW of the Middle Miocene andesitic Mátra stratovolcano (Fig. 1). This locality at the village of Tar was defined as the type-locality of the Middle Ignimbrite Unit (or 'Middle Rhyolite Tuff Horizon'; Hámor et al., 1987) in the Pannonian Basin. However, the trace element pattern of the glasses of this ignimbrite is indistinguishable from that characterizing the UIU-W ignimbrites in the BVF. This strong geochemical similarity is supported also by the mineral chemical data, i.e. composition of plagioclases and biotites. Although these pyroclastic flow deposits may have originated from different volcanic eruptions, the erupted silicic magmas should have undergone very similar petrogenetic processes. New palaeomagnetic and K/Ar data (Márton and Pécskay, 2002, personal communication) imply also a temporal correlation between these ignimbrites. Based on the sum of this evidence, it appears likely that the Tar ignimbrite belongs to the same volcanic eruption that resulted in the UIU-W pyroclastic flow deposits. This suggests a need for a reconsideration of the stratigraphic classification of the widespread Miocene silicic volcanic rocks in the Pannonian Basin. In such a correlation study, the LA-ICP-MS analysis of glasses (glass shards, and silicate melt inclusions in phenocrysts) combined with mineral chemical data would be a powerful tool.

6.2. Petrogenetic implications

The variation in trace element composition of glasses and in the chemistry of minerals implies differences in the petrogenetic evolution of the rhyolitic magmas in the Bükkalja Volcanic Field. This rhyolite volcanism was partly contemporaneous with calc-alkaline volcanic activity at the Northern Pannonian Basin. Explosive and widespread silicic magmatism often precedes or is coeval with calc-alkaline andesitic to dacitic magmatism in convergent continental margin and continental back-arc basin tectonic settings (De Silva, 1989; Gans et al., 1989; Davidson et al., 1991; Johnson, 1991; Feeley and Grunder, 1991; Siebel et al., 2001). The andesitic and rhyolitic magmas could be generated independently,

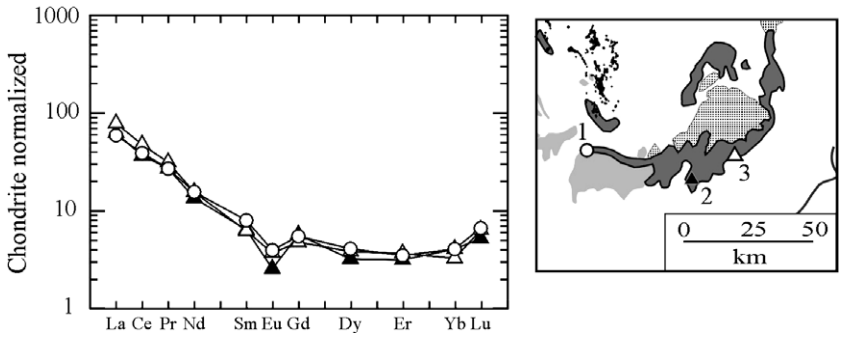

Fig. 11. Comparison of chondrite (Nakamura, 1974) normalized rare-earth element patterns of glasses of non-welded ignimbrites from the UIU-W [(2) Demjén, (3) Bogács] and from Tar, NW-Mátra (1). The Tar ignimbrite was considered previously as the type-locality of MIU (Hámor et al., 1987). However, the strong geochemical similarity with the UIU-W ignimbrites suggests a reconsideration of its stratigraphic classification.

but can also be genetically related. In general, two end-member models are proposed for the origin of Si-rich magmas that have a close relationship with geodynamic evolution. Silicic magmas can be formed by anatexis of continental crust (Reid, 1983; Huppert and Sparks, 1988; Ruiz et al., 1988; Francis et al., 1989), a process that occurs predominantly in areas with thick continental crust and typically produces large-volume ignimbrite sheets. Alternatively, silicic magmas can be generated by fractional crystallization of mantle-derived mafic or andesitic melts, combined with crustal assimilation (Bacon and Druitt, 1988, Musselwhite et al., 1989; Johnson, 1991; McCulloch et al., 1994; Siebel et al., 2001). Eruption of such small- or medium-volume ignimbrites is usually thought to take place in regions with thinner crust (Wark, 1991). The Miocene silicic ignimbrites of the Northern Pannonian Basin were formed roughly coeval with the formation of a back-arc basin area by lithospheric extension. The LIU can be considered as pre-extensional (>18 Ma), whereas the MIU and UIU are syn-extensional (18–13 Ma) volcanic suites. Thus, they were generated during a period with a transition from a thicker (>35 km) to thinner (<30 km; Tari et al., 1999) crust.

The primitive mantle-normalized trace element patterns of the glasses of the ignimbrites (Fig. 8) show some common features, such as enrichment in the LIL elements and Pb and a relative depletion in Ba, Nb, Sr and Eu. Depletion in Ba, Sr and Eu could reflect extensive feldspar fractionation. The relatively low concentration of high field strength elements (HFSE; e.g., Nb<15 ppm, Ta<1.5 ppm and Zr<100 ppm) and trace element ratios such as Ba/La (20 to 40) and La/Nb (1 to 5) suggest a subduction-related component in their genesis. However, all of these geochemical features could also be inherited in the continental crust, providing the source of the silicic magmas. Previous models usually invoked a crustal anatectic origin of the Miocene silicic magmas in the Pannonian Basin (e.g., Downes, 1996; Lexa and Konečný, 1998; Póka et al., 1998), although Harangi (2001) pointed out that variation in radiogenic isotope ratios of the pumices could only be explained by involvement of both mantle and crustal components in their genesis. Incompatible trace element ratios such as La/Nb and Th/Nb ratios are not influenced by the fractionation of feldspars and pyroxenes, and therefore they can be used to constrain the source of the magmas and/or to reveal the fractionation of minor and accessory minerals such as hornblende, biotite, ilmenite, zircon and allanite. In this plot (Fig. 12), the four main ignimbrite groups are clearly separated, suggesting a different petrogenetic evolution. The analyzed glasses of the Bükkalja ignimbrites are rhyolites with high SiO_2 content (>75 wt.%). Therefore, the differences in the trace element ratios cannot be explained by different degrees of magmatic differentiation alone. Instead, different ratios of highly incompatible trace elements could reflect compositional differences in their parental magmas and limited fractionation of specific mineral phases. The glasses of LIU and UIU define a linear trend in the La/Nb vs. Th/Nb plot spreading from the lower end of the Miocene calc-alkaline andesite field towards the higher La/Nb and Th/Nb ratios. Fractionation of hornblende, biotite and ilmenite could be responsible for this shift, whereas crystallization of zircon and allanite move the data points in the opposite direction. Petrographic observations are consistent with this scenario, because the pyroclastic rocks of the UIU-W contain hornblende and ilmenite, whereas allanite and zircon are common in the UIU-E rocks. The spread

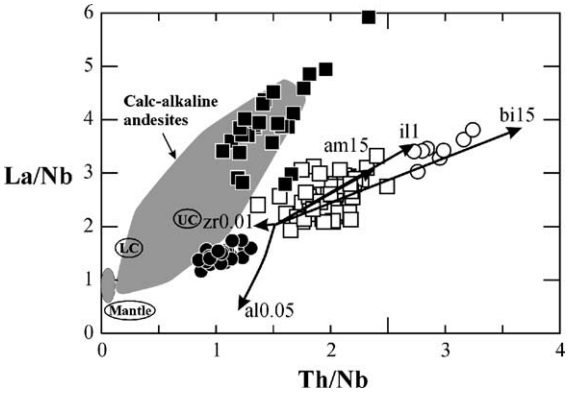

Fig. 12. La/Nb vs. Th/Nb plot for the glasses of the Bükkalja ignimbrites (symbols as in Fig. 7). Note the clear separation of the four ignimbrite units. Average crustal (LC—lower crust, UC—upper crust) values are from Taylor and McLennan (1985). Field of calc-alkaline andesites from the Northern Pannonian Basin: Harangi et al. (2001) and Harangi and Downes, unpublished data. Fractionation vectors of different minerals (zr—zircon, al—allanite, am—amphibole, il—ilmenite, bi—biotite) are based on the distribution coefficients published by Mahood and Hildreth (1983), Bacon and Druitt (1988) and Ewart and Griffin (1994). Numbers denote the amount of fractionated mineral in weight percent.

within the data of the LIU rocks could be primarily due to fractionation of biotite and zircon. This linear trend may imply also fairly similar parental magmas. However, radiogenic isotope ratios of the pumices (Harangi, 2001; Seghedi et al., 2004) do not support a common parental magma. Pumices of the UIU-W and UIU-E ignimbrites are characterized by relatively low initial $^{87}Sr/^{86}Sr$ ratios (0.707–0.708) and high initial $^{143}Nd/^{144}Nd$ ratios (0.5124–0.5125) compared with those of the LIU (0.709–0.710 and 0.51220–0.51225, respectively). This suggests an involvement of variable amounts of mantle and crustal components in the genesis of the silicic volcanic rocks of the BVF and similar sources for the silicic magmas of the two UIU ignimbrite groups. The difference in trace element composition between the two UIU groups can be explained primarily by the different fractionation paths of their magmas. Amphibole fractionation in addition to separation of plagioclase and orthopyroxene characterized the evolution of the UIU-W magmas, whereas the UIU-E rhyolites are more differentiated, where plagioclase, biotite, sanidine and accessory minerals such as allanite and zircon controlled the chemical evolution of the melt. It is remarkable that these different magma evolution processes occurred spatially very close to one another roughly at the same time (about 13.5 Ma), implying the existence of separated silicic magma chambers beneath the Northern Pannonian Basin during the Late Miocene. The compositional homogeneity of the LIU and UIU ignimbrites, irrespective of the stratigraphic position of the samples, suggests that the eruption of silicic magmas could have occurred from a homogeneous part of the magma chambers.

The glasses of the MIU shift away toward the higher La/Nb ratios from the LIU-UIU trend. This cannot be explained by fractionation of any mineral phases from a magma common with LIU or UIU, but rather suggests a different origin for the MIU silicic magma. One of the most characteristic features of the MIU rocks is the strong geochemical heterogeneity in the compositions of both the phenocrysts (plagioclase, biotite) and the glasses of fiamme and glass shards even in single samples. Furthermore, in the upper part of this volcanic suite andesitic scoriae and rhyolitic pumices, as well as banded pumices, can be found (Czuppon et al., 2001). All of these features imply a zoned magma chamber and syn-eruptive mingling of different magma batches (Harangi et al., 2002). Strong intra-sample variations of trace element composition in glasses support this suggestion. The fiamme and glass shards in these rocks could represent magma batches that have undergone different degrees of differentiation. The chemistry of the main mineral phases (e.g., plagioclase, orthopyroxene) suggests derivation of the rhyolitic melts from metaluminous andesitic parental magma. Plagioclases often show high An-content (>75 mol%), whereas orthopyroxenes are relatively Mg-rich (En=49–82 mol%; Lukács et al., 2002) and have CaO=0.5–1.7 wt.% and Al_2O_3=0.6–2.2 wt.% that are consistent with metaluminous host magma affinity based on the discrimination scheme of Maeda et al. (1991). The overlap of the trace element ratios of the MIU glasses and the calc-alkaline andesites close to the ignimbrite field could support this conclusion. The Miocene silicic volcanism was contemporaneous with the formation of the back-arc basin area, i.e. with the continuous thinning of the lithosphere. The magmagenesis of the rhyolitic magmas in the Northern Pannonian Basin, i.e. the involvement of mantle and crustal component, is consistent with this geodynamic situation.

7. Conclusions

Our new detailed geochemical study on the Miocene ignimbrite suite of the Northern Pannonian Basin suggests that the in situ trace element content of glasses, along with compositions of the main mineral phases, could be a powerful discrimination tool in the correlation of silicic pyroclastic rocks over distances of several tens of kilometres. The LA-ICP-MS analysis of glass shards with a size of only a few tens of micrometers is a rapid technique providing the concentration of a large number of trace elements with low detection limits and with minimal sample preparation. The in situ trace element data of glasses reflect the composition of the liquid part of the erupted magma and therefore provide a better geochemical fingerprint for the pyroclastic deposits than the bulk pumices, which contain also variable amounts of phenocrysts and possibly also xenocrysts. Therefore, these data can be used effectively in correlation studies, providing a more refined correlation of scattered silicic pyro-

clastic deposits than the geochronological and palaeomagnetic data.

In addition, trace element abundances of the glasses can also constrain the petrogenesis of the host silicic magmas. Based on the trace element characteristics of the glass shards and fiamme and the chemical composition of phenocrysts, we have identified at least four silicic magmatic systems that were active beneath the Northern Pannonian Basin during a continuous thinning of the crust and the lithosphere in the Miocene (21 to 13.5 Ma). The trace element composition of the erupted melts was controlled mostly by crystallization of minor and accessory minerals, such as hornblende, ilmenite, allanite and zircon. The ignimbrite precursor magmas, especially those of MIU, might have similarities with the Middle Miocene calc-alkaline andesitic magmas erupted to the north of the ignimbrite field in the Northern Pannonian Basin ('Western Carpathian Arc'), suggesting a common origin. Syn-eruptive magma mingling resulted in strong intra-sample compositional variation in the MIU pyroclastic suite. At the end of the silicic volcanic period, eruption of different kinds of rhyolitic magmas occurred contemporaneously and spatially very close to one another in the Bükkalja Volcanic Field.

Acknowledgements

We gratefully acknowledge the kind assistance of Drs. Andy Beard and Theo Ntaflos during the microprobe work. This study was carried out during Sz.H.'s stays in Utrecht supported by a Europrobe grant and a NATO fellowship, respectively. The Utrecht ICP-MS laboratory has received funding from the Netherlands Organization of Scientific Research (NWO/GOA). Constructive suggestions given by Drs. R.M. Briggs and S. De Silva helped to clarify our ideas presented in this paper.

References

Bacon, C.R., Druitt, T.H., 1988. Compositional evolution of the zoned calc-alkaline magma chamber of Mount Mazama, Crater Lake, Oregon. Contrib. Mineral. Petrol. 98, 224–256.

Bogaard, v.d.P., Schmincke, H.-U., 1985. Laacher see tephra: a widespread isochronous late quaternary tephra layer in central and northern Europe. Geol. Soc. Amer. Bull. 96, 1554–1571.

Bryant, C.J., Arculus, R.J., Eggins, S.M., 1999. Laser ablation-inductively coupled plasma-mass spectrometry and tephras: a new approach to understanding arc-magma genesis. Geology 27, 1119–1122.

Capaccioni, B., Coradossi, N., Harangi, R., Harangi, S., Karátson, D., Sarocchi, D., Valentini, L., 1995. Early Miocene Pyroclastc Rocks of the Bükkalja Ignimbrite Field (North Hungary)—A Preliminary Stratigraphic Report. In: Downes, H., Vaselli, O. (Eds.), Neogene and related volcanism in the Carpatho–Pannonian Region, Acta Vulcanol., vol. 7, pp. 119–124.

Chesner, C.A., 1998. Petrogenesis of the Toba Tuffs, Sumatra, Indonesia. J. Petrol. 39 (3), 397–438.

Clift, P., Blusztajn, J., 1999. The trace element characteristics of aegean and aeolian volcanic arc marine tephra. J. Volcanol. Geotherm. Res. 92, 321–347.

Csontos, L., Nagymarosy, A., Horváth, F., Kovác, M., 1992. Tertiary evolution of the Intra-Carpathian area: a model. In: Ziegler, P.A. (Ed.), Geodynamics of Rifting, vol. I. Case Studies on Rifts: Europe and Asia, Tectonophysics, vol. 208, pp. 221–241.

Czuppon, Gy., Harangi, Sz., Ntaflos, T., Lukács, R., Szabó, Cs., Koller, F., 2001. Mixed andesite-rhyolite ignimbrite from the Miocene Bükkalja Ignimbrite Volcanic Field, Northern Hungary: evidence for magma mixing. Mitt. Osterr. Mineral. Ges. 146, 61–63.

Davidson, J.P., Harmon, S.R., Wörner, G., 1991. The source of central Andean magmas: some considerations. In: Harmon, R.S., Rapela, C.W. (Eds.), Andean Magmatism and its Tectonic Setting, Geol. Soc. Am. Spec. Pap., vol. 265, pp. 233–243.

De Silva, S.L., 1989. The Altiplano–Puna volcanic complex of the central Andes. Geology 17, 1102–1106.

De Silva, S.L., Francis, P.W., 1989. Correlation of large ignimbrites—two case studies from the Central Andes of Northern Chile. J. Volcanol. Geotherm. Res. 37, 133–149.

Downes, H., 1996. Neogene magmatism and tectonics in the Carpatho–Pannonian region. In: Decker, K. (Ed.), PANCARDI Workshop 1996, Dynamics of the Pannonian–Carpathian–Dinaride System, Mid. Ges. Geol. Bergbaustud. Österr., vol. 41, pp. 104–105.

Embey-Isztin, A., Dobosi, G., 1995. Mantle source characteristics for miocene–pleistocene alkali basalts, Carpathian–Pannonian Region: a review of trace elements and isotopic composition. In: Downes, H., Vaselli, O. (Eds.), Neogene and Related Volcanism in the Carpatho–Pannonian Region, Acta Vulcanol., vol. 7, pp. 155–166.

Embey-Isztin, A., Downes, H., James, D.E., Upton, B.G.J., Dobosi, G., Ingram, G.A., Harmon, R.S., Scharbert, H.G., 1993. The petrogenesis of pliocene alkaline volcanic rocks from the Pannonian Basin, Eastern Central Europe. J. Petrol. 34, 317–343.

Ewart, A., Griffin, W.L., 1994. Application of proton-microprobe data to trace-element partitioning in volcanic rocks. Chem. Geol. 117, 251–284.

Feeley, T.C., Grunder, A.L., 1991. Mantle contribution to the evolution of middle tertiary silicic magmatism during early

stages of extension: the Egan Range volcanic complex, east-central Nevada. Contrib. Mineral. Petrol. 106, 154–169.

Fodor, L., Csontos, L., Bada, G., Györfi, I., Benkovics, L., 1999. Tertiary tectonic evolution of the Pannonian basin system and neighbouring orogens: a new synthesis of palaeostress data. In: Durand, B., Jolivet, L., Horváth, F., Séranne, M. (Eds.), The Mediterranean Basins: Tertiary Extension Within the Alpine Orogen, Geol. Soc. London, Spec. Pub., vol. 156, pp. 295–334.

Francis, P.W., Sparks, R.S.J., Hawkesworth, C.J., Thorpe, R.S., Pyle, D.M., Tait, S.R., 1989. Petrology and geochemistry of volcanic rocks of the Cerro Galan caldera, N.W. Argentina. Geol. Mag. 126, 515–547.

Froggatt, T.C., 1983. Toward comprehensive upper quaternary tephra and ignimbrite stratigraphy in New Zealand using electron microprobe analysis of glass shards. Quat. Res. 19, 188–200.

Froggatt, T.C., Lowe, D.J., 1990. A review of late quaternary silicic and some other tephra formations from New Zealand: their stratigraphy, nomenclature, distribution, volume and age. N.Z. J. Geol. Geophys. 33, 89–109.

Gans, P.B., Mahood, G.A., Schermer, E., 1989. Synextensional magmatism in the Basin and Range Province: a case study from the eastern Great Basin. Spec. Pap.-Geol. Soc. Am. 233 1–53.

Günther, D., 2001. Quantitative fluid inclusion analysis using a 193 nm excimer laser ablation system coupled to ICP-MS. In: Sylvester, P. (Ed.), Laser-ablation-ICPMS in the Earth Sciences. Principles and Applications, Mineralogical Associations of Canada Short Course Series, vol. 21, pp. 47–61.

Hámor, G., Balogh, K., Ravaszné Baranyai, L., 1987. Az észak-magyarországi harmadidõszaki formációk radiometrikus kora. Földt. Intéz. Évi Jel. 1986-ról, 61–76.

Harangi, Sz., 2001. Neogene to quaternary volcanism of the Carpathian–Pannonian Region—a review. Acta Geol. Hung. 44, 223–258.

Harangi, Sz., Downes, H., Kósa, L., Szabó, Cs., Thirlwall, M.F., Mason, P.R.D., Mattey, D., 2001. Almandine garnet in calc-alkaline volcanic rocks of the Northern Pannonian Basin (Eastern-Central Europe): geochemistry, petrogenesis and geodynamic implications. J. Petrol. 42, 1813–1843.

Harangi, Sz., Lukács, R., Czuppon, Gy., Szabó, Cs., 2002. Magma mixing in a compositionally layered magma chamber: a silicate melt inclusion study. Workshop on Volcanic Systems, Seiano, Italy, Proceedings, pp. 101–106.

Hildreth, W., 1981. Gradients in silicic magma chambers: implications for lithospheric magmatism. J. Geophys. Res. 86, 10153–10192.

Hildreth, W., Mahood, G., 1985. Correlation of ash-flow tuffs. Geol. Soc. Amer. Bull. 96, 968–974.

Horváth, F., 1993. Towards a mechanical model for the formation of the Pannonian basin. Tectonophysics 226, 333–357.

Horváth, F., Berckhemer, H., 1982. Mediterranean back arc basins. In: Berckhemer, H., Hsü, K. (Eds.), Alpine-Mediterranean Geodynamics, Amer. Geophys. Union Geol. Soc. Amer., Geodynamic Series, vol. 7, pp. 141–173.

Huppert, H.E., Sparks, R.S.J., 1988. The generation of granitic magmas by intrusion of basalt into continental crust. J. Petrol. 29, 599–624.

Johnson, C.M., 1991. Large-scale crust formation and lithosphere modification beneath middle to late cenozoic calderas and volcanic fields, Western North America. J. Geophys. Res. 96, 13485–13507.

Konečný, V., Lexa, J., Hojstricová, V., 1995. The Central Slovakia Neogene volcanic field: a review. In: Downes, H., Vaselli, O. (Eds.), Neogene and Related Magmatism in the Carpatho–Pannonian Region, Acta Vulcanol., vol. 7, pp. 63–78.

Lexa, J., Konečný, V., 1998. Geodynamic aspects of the neogene to quaternary volcanism. In: Rakús, M. (Ed.), Geodynamic Development of the Western Carpathians, Geol. Surv. Slovak Republik, Bratislava, pp. 219–240.

Lowe, D.J., Newnham, R.M., Ward, C.M., 1999. Stratigraphy and chronology of a 15 ka sequence of multi-sourced silicic tephras in a montane peat bog, eastern North Island, New Zealand. N.Z. J. Geol. Geophys. 42, 565–579.

Lukács, R., Czuppon, G., Harangi, S., Szabó, C., Ntaflos, T., Koller, F., 2002. Silicate melt inclusions in ignimbrites, Bükkalja Volcanic Field, Northern Hungary—texture and geochemistry. Acta Geol. Hung. 45 (4), 341–358.

Maeda, J., Shimura, T., Arita, K., Osanai, Y., Maruta, M., Bamba, M., Suetake, S., 1991. Chemical features of orthopyroxene in peraluminous igneous rocks. Am. Mineral. 76, 1674–1682.

Mahood, G.A., Hildreth, E.W., 1983. Large partition coefficients for trace elements in high-silica rhyolites. Geochim. Cosmochim. Acta 47, 11–30.

Márton, E., Fodor, L., 1995. Combination of paleomagnetic and stress data—a case study from North Hungary. Tectonophysics 242, 99–114.

Márton, E., Pécskay, Z., 1998. Complex evaluation of paleomagnetic and K/Ar isotope data of the miocene ignimbritic volcanics in the Bükk Foreland, Hungary. Acta Geol. Hung. 41, 467–476.

Mason, P.R.D., Kraan, W.J., 2002. Attenuation of spectral interferences during laser ablation inductively coupled plasma mass spectrometry (LA-ICP-MS) using an rf only collision and reaction cell. J. Anal. At. Spectrom. 17, 858–867.

Mason, P.R.D., Downes, H., Thirlwall, M., Seghedi, I., Szakács, A., Lowry, D., Mattey, D., 1996. Crustal assimilation as a major petrogenetic process in east Carpathian Neogene to Quaternary continental margin arc magmas. J. Petrol. 37, 927–959.

Mason, P.R.D., Seghedi, I., Szakács, A., Downes, H., 1998. Magmatic constraints on geodynamic models of subduction in the Eastern Carpathians, Romania. Tectonophysics 297, 157–176.

McCulloch, M.T., Kysler, T.K., Woodhead, J.D., Kinsley, L., 1994. Pb–Sr–Nd–O isotopic constraints on the origin of rhyolites from the Taupo Volcanic Zone of New Zealand: evidence for assimilation followed by fractionation from basalt. Contrib. Mineral. Petrol. 115, 303–312.

Musselwhite, D.S., DePaolo, D.J., McCurry, M., 1989. The evolution of a silicic magma system: isotopic and chemical evidence from the Woods Mountains Volcanic Center, eastern California. Contrib. Mineral. Petrol. 101, 19–29.

Nakamura, N., 1974. Determination of REE, Ba, Mg, Na and K in carbonaceous and ordinary chondrites. Geochim. Cosmochim. Acta 38, 757–775.

Pantó, G., 1963. Ignimbrites of Hungary with regard to the genetics and classification. Bull. Volcanol. 25, 175–181.

Pearce, N.J.G., Perkins, W.T., Westgate, J.A., Gorton, M.P., Jackson, S.E., Neal, C.R., Chenery, S.P., 1997. A compilation of new and published major and trace element data for NIST SRM 610 and NIST SRM 612 glass reference materials. Geostand. Newsl. 21, 115–144.

Pearce, N.J.G., Westgate, J.A., Perkins, W.T., Eastwood, W.J., Shane, P., 1999. The application of laser ablation ICP-MS to the analysis of volcanic glass shards from tephra deposits: bulk glass and single shard analysis. Glob. Planet. Change 21, 151–171.

Pearce, N.J.G., Eastwood, W.J., Westgate, J.A., Perkins, W.T., 2002. Trace-element composition of single glass shards in distal Minoan tephra from SW Turkey. J. Geol. Soc. (Lond.) 159, 545–556.

Pécskay, Z., Lexa, J., Szakács A., Balogh, K., Seghedi, I., Konečny, V., Kovács, M., Márton, E., Kaliciak, M., Széky-Fux, V., Póka, T., Gyarmati, P., Edelstein, O., Rosu, E., Zec, B., 1995. Space and time distribution of Neogene–Quatenary volcanism in the Carpatho–Pannonian Region. In: Downes, H., Vaselli, O. (Eds.), Neogene and Related Volcanism in the Carpatho–Pannonian Region, Acta Vulcanologica, pp. 15–28.

Póka, T., Zelenka, T., Szakács, A., Seghedi, I., Nagy, G., Simonits, A., 1998. Petrology and geochemistry of the miocene acidic explosive volcanism of the Bükk Foreland; Pannonian Basin, Hungary. Acta Geol. Hung. 41, 437–466.

Reid, F.W., 1983. Origin of the rhyolitic rocks of the Taupo Volcanic Zone. J. Volcanol. Geotherm. Res. 15, 315–338.

Royden, L.H., Horváth, F., Burchfiel, B.C., 1982. Transform faulting, extension and subduction in the Carpathian–Pannonian region. Geol. Soc. Amer. Bull. 93, 717–725.

Ruiz, J., Patchett, P.J., Arculus, R.J., 1988. Nd–Sr isotope composition of the lower crustal xenoliths, evidence for the origin of mid-Tertiary felsic volcanics in Mexico. Contrib. Mineral. Petrol. 99, 36–42.

Sarna-Wojcicki, A.M., Bowman, H.R., Meyer, C.E., Russell, P.C., Woodward, M.J., McCoy, G., Rowe, J.J., Baedecker, P.A., Asaro, F., Michael, H., 1984. Chemical analyses, correlations, and ages of Upper Pliocene and Pleistocene ash layers of east-central and southern California. U. S. Geol. Surv. Prof. Pap. 1293, 1–40.

Sarna-Wojcicki, A.M., Morrison, S.D., Meyer, C.E., Hillhouse, J.W., 1987. Correlations of upper cenozoic tephra layers between sediments of the Western United States and Eastern Pacific Ocean and comparison with biostratigraphic and magnetostratigraphic age data. Geol. Soc. Amer. Bull. 98, 207–223.

Seghedi, I., Balintoni, I., Szakacs, A., 1998. Interplay of tectonics and neogene post-collisional magmatism in the intracarpathian region. Lithos 45 (1–4), 483–497.

Seghedi, I., Downes, H., Szakacs, A., Mason, P.R.D., Thirlwall, M.F., Rosu, E., Pecskay, Z., Marton, E., Panaiotu, C., 2004. Neogene–Quaternary magmatism and geodynamics in the Carpathian–Pannonian region: a synthesis. Lithos 72 (3–4), 117–146.

Shane, P.A.R., 2000. Tephrochronology: a New Zealand case study. Earth-Sci. Rev. 49, 223–259.

Shane, P.A.R., Froggatt, P.C., 1991. Glass chemistry, paleomagnetism, and correlation of middle pleistocene tuffs in southern North Island, New Zealand, and Western Pacific. N.Z. J. Geol. Geophys. 34, 203–211.

Shane, P.A.R., Froggatt, P.C., 1994. Discriminant function analysis of glass chemistry of New Zealand and North American tephra deposits. Quat. Res. 41, 70–81.

Shane, P.A.R., Smith, V., Nairn, I.A., 2003. Biotite composition as a tool for the identification of quaternary tephra beds. Quat. Res. 59, 262–270.

Siebel, W., Schnurr, W.B.W., Hahne, K., Kraemer, B., Trumbull, R.B., Bogaard, P., Emmermann, R., 2001. Geochemistry and isotope systematics of small- to medium-volume Neogene–Quaternary ignimbrites in the southern central Andes: evidence for derivation from andesitic magma sources. Chem. Geol. 171, 213–237.

Smith, L.R., 1960. Zones and zonal variations in welded ash flows. U. S. Geol. Surv. Prof. Pap. 354-F, 149–159.

Stokes, S., Lowe, D.J., 1988. Discriminant function analysis of late quaternary tephras from five volcanoes in New Zealand using glass shard major element chemistry. Quat. Res. 30, 270–283.

Stokes, S., Lowe, D.J., Froggatt, P.C., 1992. Discriminant function analysis and correlation of late quaternary tephra deposits from Taupo and Okataiana volcanoes, New Zealand, using glass shard major element composition. Quat. Int. 13/14, 103–120.

Sun, S.S., McDonough, W.F., 1989. Chemical and isotopic systematics of oceanic basalts: implications for mantle composition and processes. In: Saunders, A.D., Norry, M.J. (Eds.), Magmatism in the Oceanic Basins, Geol. Soc. London Spec. Publ., vol. 42, pp. 313–345.

Sylvester, P. (Ed.), 2001. Laser-ablation-ICPMS in the Earth Sciences. Principles and Applications, Mineralogical Associations of Canada Short Course Series, vol. 21.

Szabo, C., Harangi, S., Csontos, L., 1992. Review of neogene and quaternary volcanism of the Carpathian–Pannonian region. Tectonophysics 208 (1–3), 243–256.

Szakács, A., Zelenka, T., Márton, E., Pécskay, Z., Póka, T., Seghedi, I., 1998. Miocene acidic explosive volcanism in the Bükk Foreland, Hungary: identifying eruptive sequences and searching for source locations. Acta Geol. Hung. 41, 413–435.

Tari, G., Dövényi, P., Horváth, F., Dunkl, I., Lenkey, L., Stefanescu, M., Szafián, P., Tóth, T., 1999. Lithospheric structure of the Pannonian basin derived from seismic, gravity and geothermal data. In: Durand, B., Jolivet, L., Horváth, F., Séranne, M. (Eds.), The Mediterranean Basins: Tertiary Extension Within the Alpine Orogen, Geol. Soc. London, Spec. Publ., vol. 156, pp. 215–250.

Taylor, S.R., McLennan, S.M., 1985. The Continental Crust: its composition and Evolution. Blackwell Sci. Publ., Oxford.

Thorarinsson, S., 1944. Tefrokronologiska studier pa Island. Geogr. Ann., 1–203.

Thorarinsson, S., 1974. The terms tephra and tephrochronology. In: Westgate, J.A., Gold, C.M. (Eds.), World Bibliography and Index of Quaternary Tephrochronology. University of Alberta, Alberta, pp. xvii–xviii.

Tomek, C., Hall, J., 1993. Subducted continental margin image in the Carpathians of Czechoslovakia. Geology 21, 535–538.
Varga, Gy., 1981. Újabb adatok az összesült tufatelepek és ignimbritek ismeretéhez. MÁFI Évi Jel. 1979-ről, 499–509.
Wark, D.A., 1991. Oligocene ash flow volcanism, Northern Sierra Madre Occidental: role of mafic and intermediate-composition magmas in rhyolite genesis. J. Geophys. Res. 96, 13389–13411.
Westgate, J.A., Gorton, M.P., 1981. Correlation techniques in tephra studies. In: Self, S., Sparks, R.S.J. (Eds.), Tephra Studies. Reidel, Dordrecht, pp. 73–94.
Westgate, J.A., Perkins, W.T., Fuge, R., Pearce, N.J.G., Wintle, A.G., 1994. Trace element analysis of volcanic glass shards by laser ablation inductively coupled plasma mass spectrometry: application to quaternary tephro-chronological studies. Appl. Geochem. 9, 323–335.
Westgate, J.A., Shane, P.A.R., Pearce, N.J.G., Perkins, W.T., Korisettar, R., Chesner, C.A., Williams, M.A.J., Acharyya, S.K., 1998. All toba tephra occurrences across Peninsular India belong to the 75,000 yr B. P. eruption. Quat. Res. 50, 107–112.
Wortel, M.J.R., Spakman, W., 2000. Subduction and slab detachment in the Mediterranean–Carpathian Region. Science 290, 1910–1917.